www.sciencemag.org/content/355/6323/374/suppl/DC1

Supplementary Materials for

Synthesis and characterization of the pentazolate anion *cyclo*-N_5^- in $(N_5)_6(H_3O)_3(NH_4)_4Cl$

Chong Zhang, Chengguo Sun, Bingcheng Hu,* Chuanming Yu, Ming Lu*

*Corresponding author. Email: hubc@njust.edu.cn (B.H.); luming@mail.njust.edu.cn (M.L.)

Published 27 January 2017, *Science* **355**, 374 (2017)
DOI: 10.1126/science.aah3840

This PDF file includes:

S1 Synthetic details and characterization of products

S1.1 General information

All reagents and solvents used were of analytical grade. 2,6-dimethyl-4-amino-phenol was produced according to the methods described in the literature (*30*). Electrospray ionization (ESI) mass spectra were recorded on a Finnigan TSQ Quantum ultra AM mass spectrometer. The samples were dissolved in methanol, and infused via a syringe pump a 5 μL/min. The instrument was run in the negative ion mode with the capillary voltage at −3000 V and the dissociation potential (source CID) at −20 V. In the MS/MS mode, the quadrupole mass analyzer was set to pass the parent ion at unit mass resolution using Ar as the collision gas. NMR spectra were obtained on a Bruker Avance III 500 MHz instrument equipped with Magnex Scientific superconducting magnets. ^{1}H NMR spectrum was referenced to tetramethylsilane (0 ppm), and ^{15}N NMR spectra were referenced externally to neat CH_3NO_2 (0 ppm). FT-IR spectra were recorded on a Thermo Nicolet IS10 instrument. Raman spectra were measured with a Renishaw (inVia) Raman spectrometer (785 nm excitation). TG-DSC-DTG-MS-IR measurements were performed on a Netzsch STA 409 PC/PG thermal analyzer coupled to a Thermo Nicolet IZ10 FTIR spectrometer equipped with a TG-MS-IR gas cell at a heating rate of 10 K/min under nitrogen (argon) atmosphere.

S1.2 Synthesis of 3,5-dimethyl-4-hydroxyphenylpentazole (HPP)

The synthesis of HPP and its ^{15}N-labeled compounds was performed according to our previous report (*17*), and the corresponding synthetic routes were described in Figure S1.

S1.3 Synthesis of pentazolate salt

An aqueous solution of ferrous bisglycinate (2.65 g, 13 mmol) was added to a solution of HPP (0.993 g, 5.2 mmol) in a mixture of solvents (160 mL) of acetonitrile and methanol (v/v, 1/1) and stirred at −45 °C for 30 min. A cold methanol solution of *m*-chloroperbenzoic acid (4.26 g, 21mmol) was added. The reaction mixture was stirred at −45 °C for more than 24 h, the insoluble materials were eliminated by filtration. The

collected filtrate was evaporated under vacuum to furnish a dark-brown solid. The pure product could be isolated through a column of silica gel (ethyl acetate/ethanol, 10/1) with an acceptable yield (19%, based on the number of moles of HPP) of $(N_5)_6(H_3O)_3(NH_4)_4Cl$ as an air-stable white solid.

^{1}H NMR (DMSO-d_6, TMS): δ 7.17 ppm (s). ^{15}N NMR (DMSO-d_6, $MeNO_2$): δ −356.18 ppm (s). IR: 3132 (m), 3020 (s), 2917 (m), 2827 (m), 2036 (w), 1696 (w), 1490 (w), 1418 (s), 1224 (s), 1015 (w), 950 (w) cm^{-1}. Raman: 1428, 1184, 1117, 1021 cm^{-1}.

S1.4 Synthetic routes of pentazolate salts

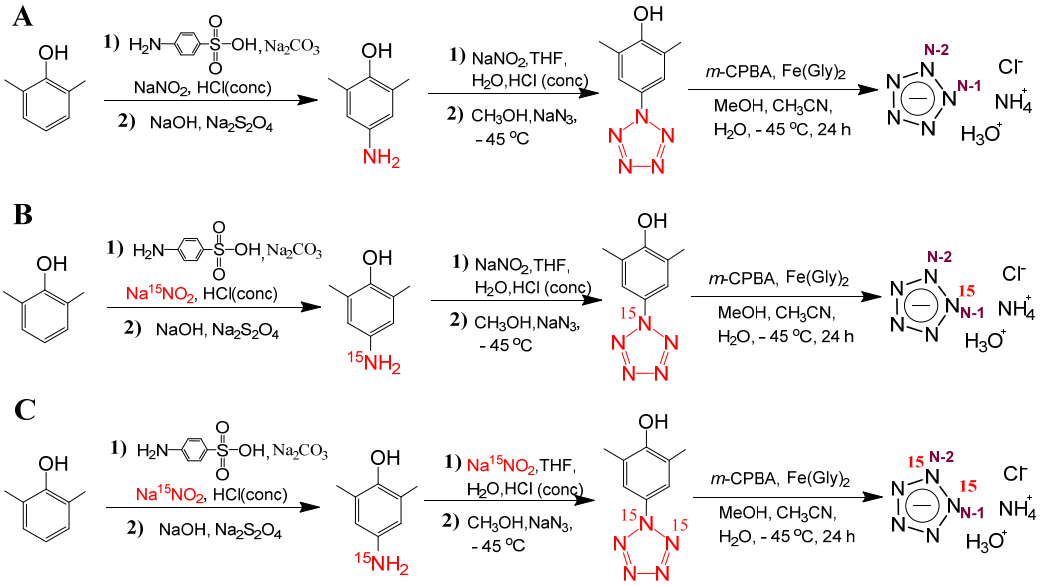

Figure S1 Synthesis of pentazolate salts.

S1.5 Electrospray Ionization (ESI) Mass Spectrometry

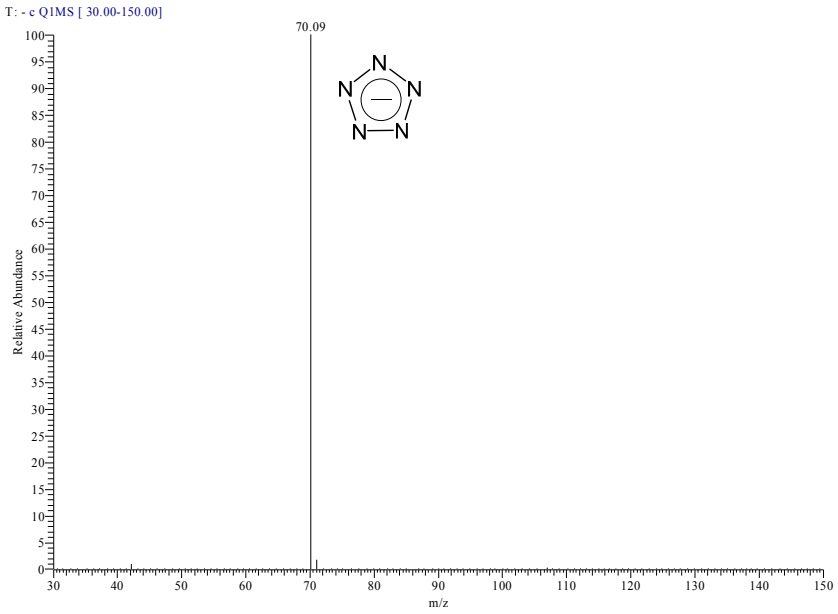

Figure S2: The mass spectrum of *cyclo*-N_5^- (*m/z* of 70).

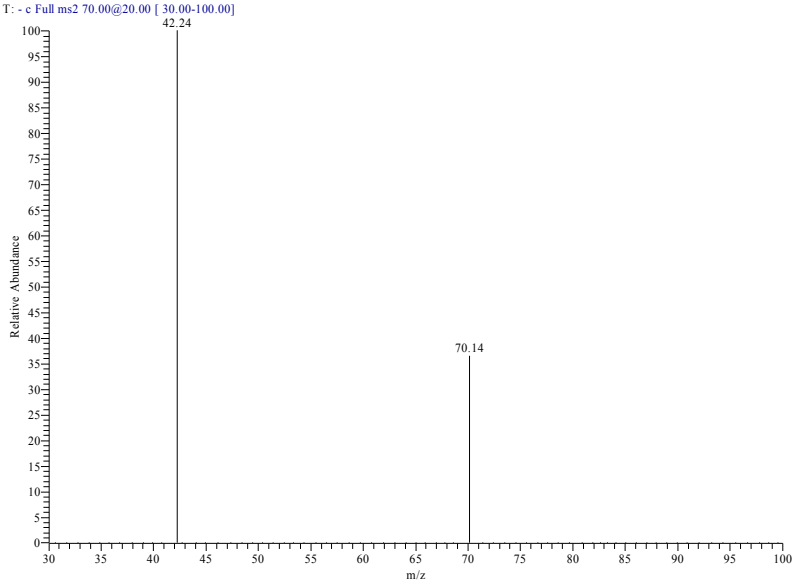

Figure S3: The mass spectrum of fragmentation of *cyclo*-N_5^- (*m/z* of 70) at low collision energy (20 eV).

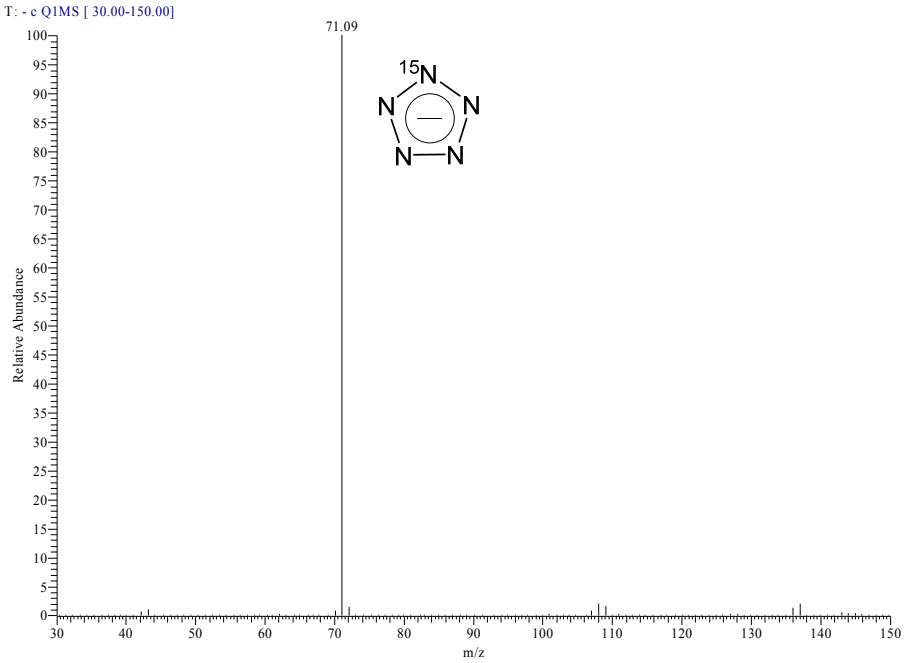

Figure S4: The mass spectrum of *cyclo*-N_5^- (*m/z* of 71), labeled ^{15}N atom at N-1 position.

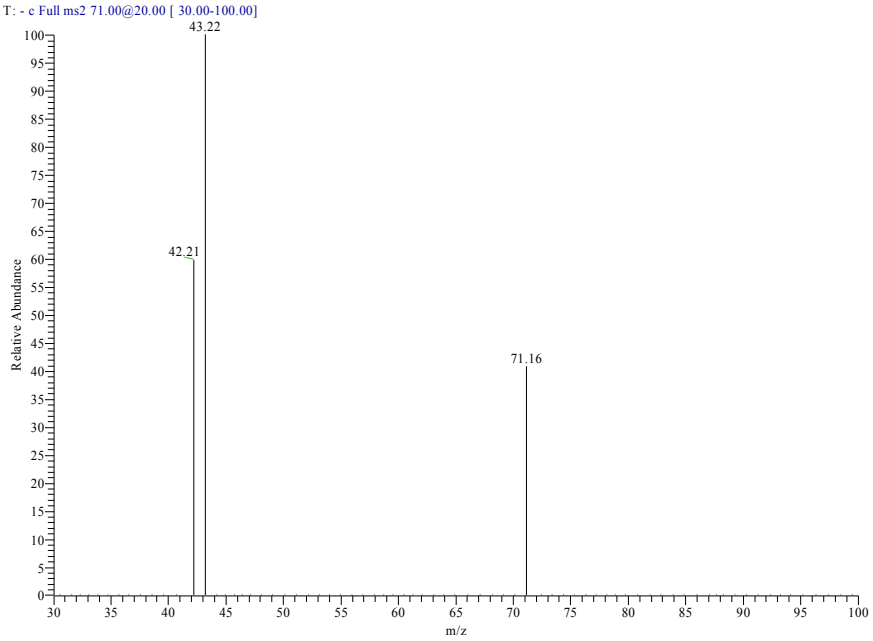

Figure S5: The mass spectrum of fragmentation of *cyclo*-N_5^- (*m/z* of 71), labeled ^{15}N atom at N-1 position at low collision energy (20 eV).

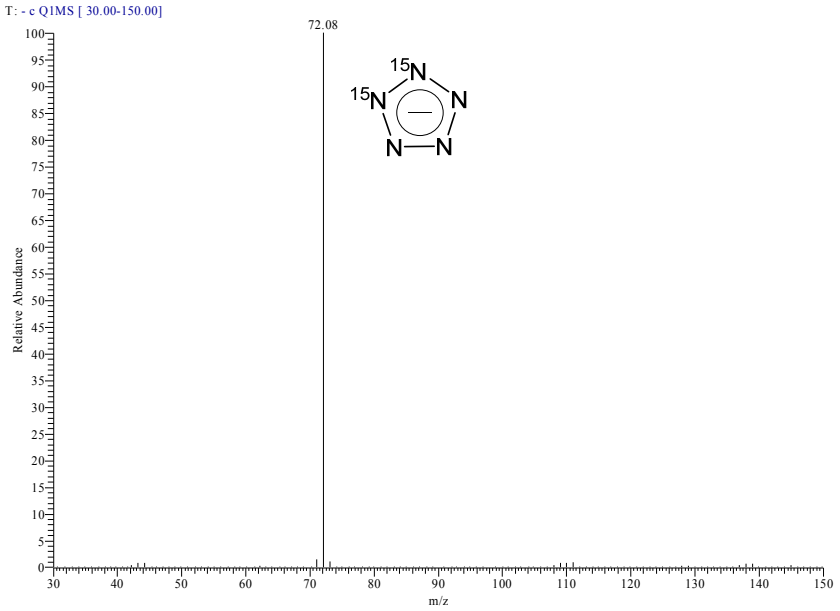

Figure S6: The mass spectrum of *cyclo*-N_5^- (*m/z* of 72), labeled ^{15}N atom at N-1 and N-2 positions.

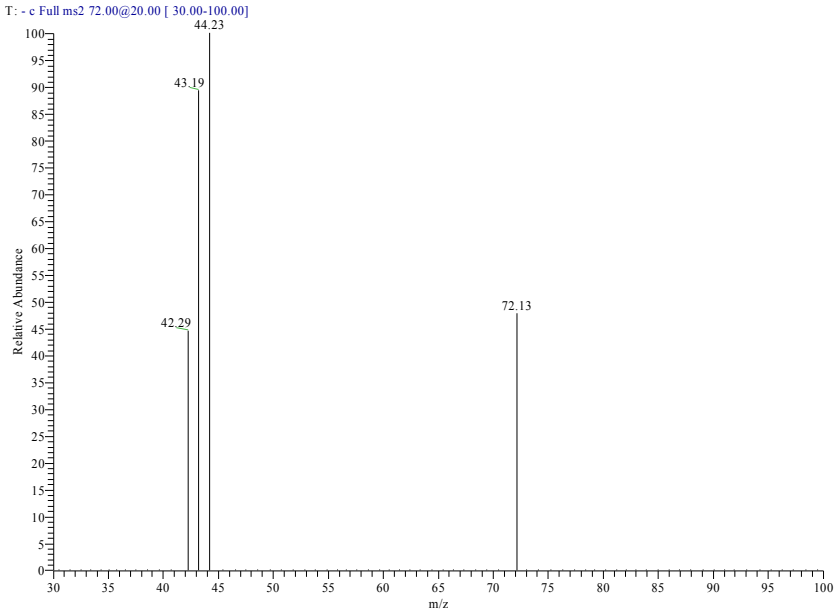

Figure S7: The mass spectrum of fragmentation of *cyclo*-N_5^- (*m/z* of 72), labeled ^{15}N atom at N-1 and N-2 positions at low collision energy (20 eV).

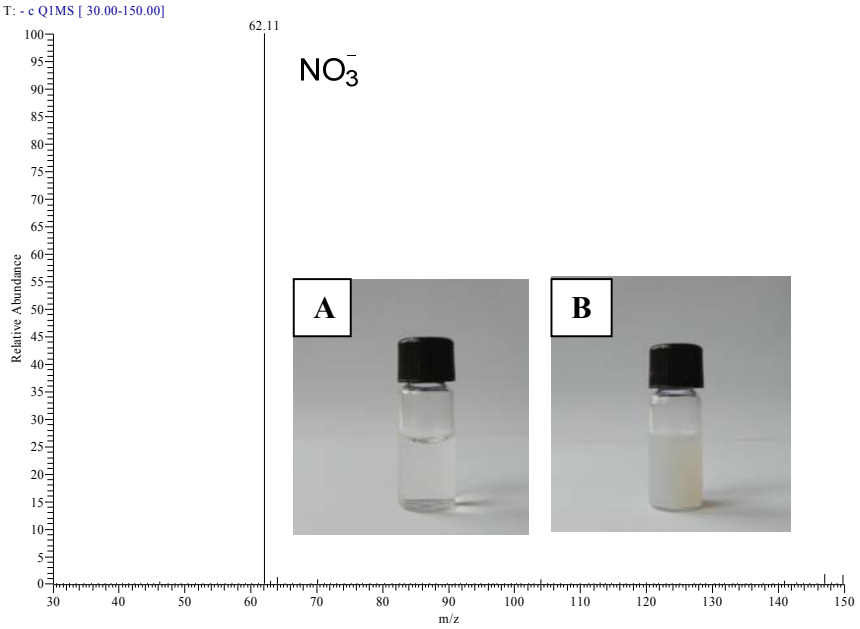

Figure S8: The mass spectrum of aqueous solution of pentazolate salt after treating with silver nitrate. (**A**) The aqueous solution of pentazolate salt; (**B**) The aqueous solution of pentazolate salt after treating with silver nitrate.

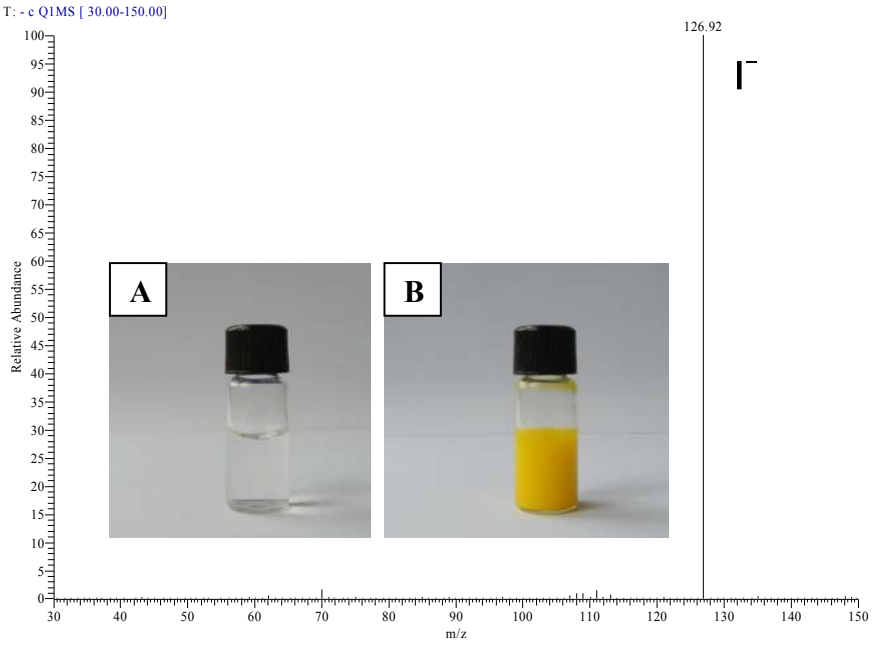

Figure S9: The mass spectrum of aqueous solution of pentazolate salt after treating with Nessler's reagent. (**A**) The aqueous solution of pentazolate salt; (**B**) The aqueous solution of pentazolate salt after treating with Nessler's reagent.

S1.6 ^{1}H NMR Spectrum

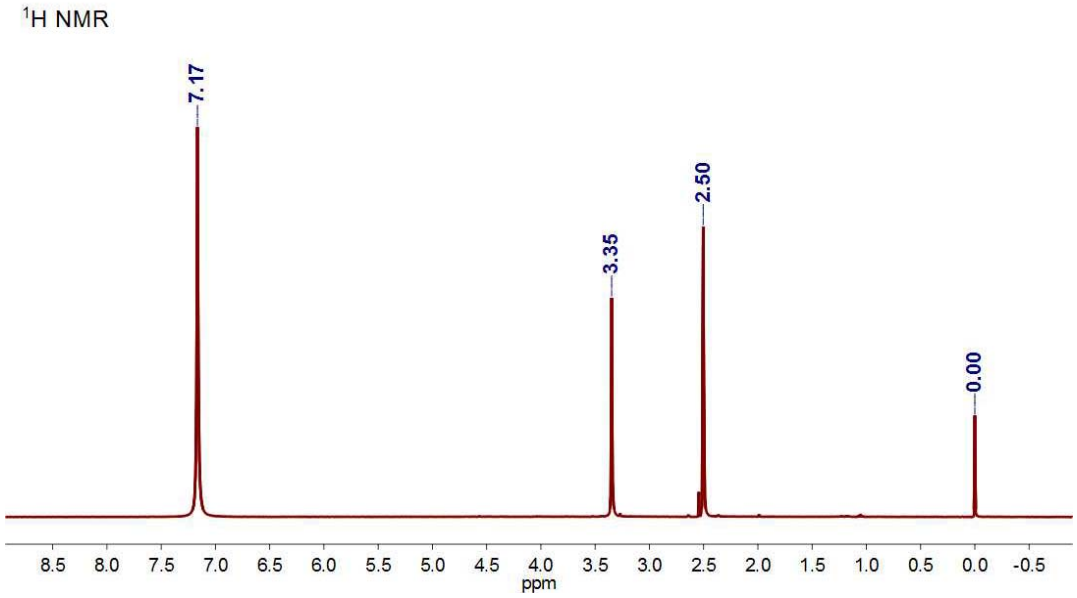

Figure S10: ^{1}H NMR spectrum of $(N_5)_6(H_3O)_3(NH_4)_4Cl$ in DMSO.

S1.7 Decomposition process of pentazolate salt according to thermal analysis

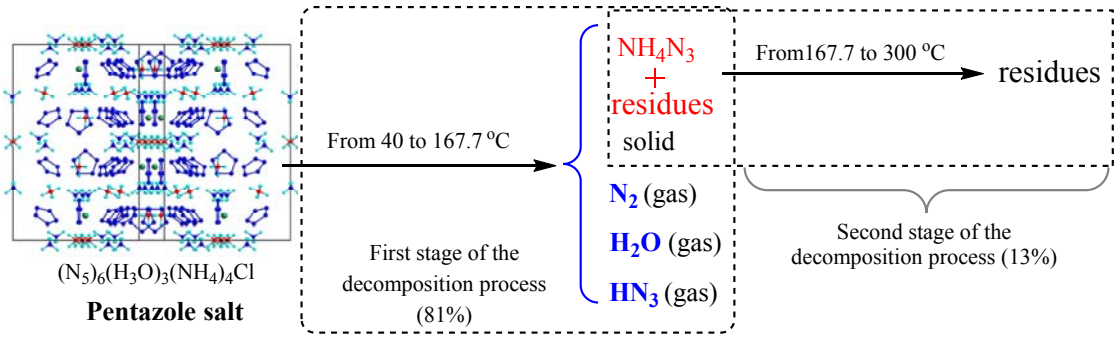

Figure S11: The proposed thermal decomposition process of $(N_5)_6(H_3O)_3(NH_4)_4Cl$.

S1.8 Mass spectra of TG-DSC-DTG-MS-IR

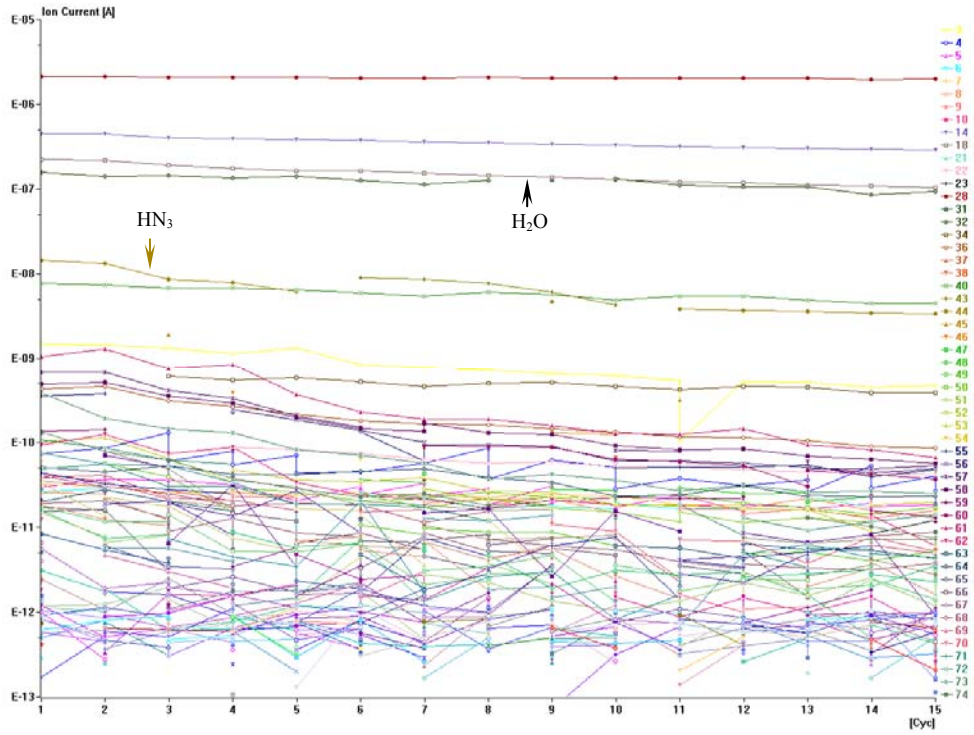

Figure S12: The mass spectra of full scan of the gas products obtained from the thermal decomposition of the $(N_5)_6(H_3O)_3(NH_4)_4Cl$ under nitrogen.

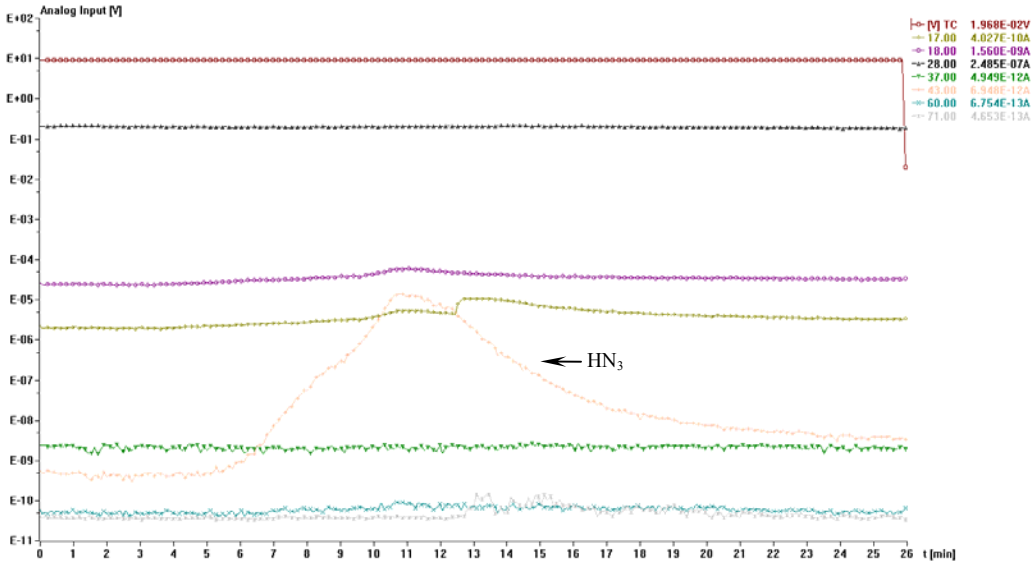

Figure S13: The mass spectra of selected ion monitoring scan of the gas products obtained from the thermal decomposition of the $(N_5)_6(H_3O)_3(NH_4)_4Cl$ under argon.

S1.9 Infrared Spectrum

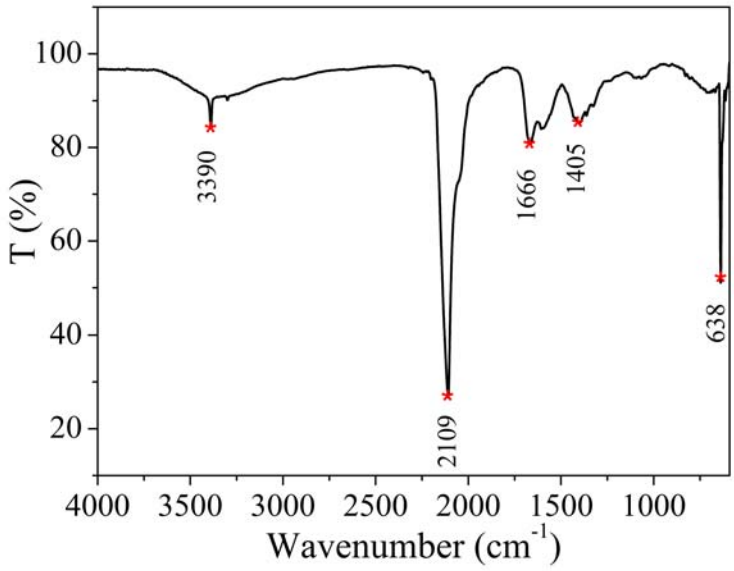

Figure S14: The infrared spectrum of residues formed at the first stage of the decomposition process of pentazolate salt.

S2 X-ray Diffraction Studies

Colorless crystals of pentazolate salt suitable for single crystal X-ray diffraction were grown by dissolving the solid in a minimum amount of the mixed solution of ethanol (C_2H_5OH 95%) and ethyl acetate and holding at −18 °C for two weeks. All data were collected with a Bruker D8 Venture single-crystal diffractometer (Cu *Kα*, λ = 1.54178 Å). The corresponding data were collected with Bruker APEX2 program and reduced with Bruker SAINT program. Absorption correction was performed by semi-empirical method implemented in SADABS. The structure was solved by direct methods with SHELXT program (*31*) and refined by least-square methods with SHELXL-2014 program (*32, 33*) contained in OLEX2 suite (*34*). The non-hydrogen atoms were identified by SHELXT program directly and refined anisotropically. The hydrogen atoms were located from difference Fourier map inspection and freely refined with Uiso(H) = 1.5Ueq (N, O). Relevant crystal data and refinement results are summarized in **Table S1**.

Table S1: Crystallographic Data for $(N_5)_6(H_3O)_3(NH_4)_4Cl$.

$N_{34}H_{25}O_3Cl$	
Formula	$(N_5)_6(H_3O)_3(NH_4)_4Cl$
Formula weight	584.99 $g \cdot mol^{-1}$
Temperature	123 K
Wavelength	1.54178 Å
Crystal system	cubic
Space group	*Fd*-3*m*
Cell parameters	$a=b=c=17.9681(5)$Å
	$\alpha=\beta=\gamma=90°$
Cell volume	5801.0(5) $Å^3$
Formula Z	8
Calc. density	1.340 $g \cdot cm^{-3}$
Absorption coefficient	1.800 mm^{-1}
F(000)	2432
Crystal size	0.20 × 0.20 × 0.25 mm
Theta range for data collection	4.262 to 66.372 °
Limiting indices	-21<=h<=19, -21<=k<=21, -21<=l<=21
Reflections collected / unique	22726 / 279 [R(int) = 0.0337]
Absorption correction	Semi-empirical from equivalents
Max. and min. transmission	0.1665 and 0.0682
Refinement method	Full-matrix least-squares on F^2
Goodness-of-fit on F^2	1.208
Final R indices [I>2sigma(I)]	$R_1 = 0.0580$, $wR_2 = 0.1663$
R indices(all data)	$R_1 = 0.0580$, $wR_2 = 0.1663$
Largest diff. peak and hole	0.523 and -0.940 $e \cdot Å^{-3}$
CSD	431382

Table S2: Bond lengths.

parameter	bond length(Å)	parameter	bond length(Å)
O(2)-H(2)	0.83(2)	N(2)-N(1)	1.324(4)
O(1)-H(1)	0.84(2)	N(1)-N(1)#1	1.309(5)
N(3)-N(2)	1.310(3)	N(4)-H(4A)	0.82(2)
N(3)-N(2)#1	1.310(3)	N(4)-H(4B)	0.83(2)

Symmetry code: #1: 1.75-x, 1.75-y, z

Table S3: Bond angles.

parameter	bond angle(°)	parameter	bond angle(°)
N(2)-N(3)-N(2)#1	107.8(3)	N(1)#1-N(1)-N(2)	107.8(2)
N(3)-N(2)-N(1)	108.3(3)	H(4A)-N(4)-H(4B)	113(2)

Symmetry code: #1: 1.75-x, 1.75-y, z

Table S4: Hydrogen bonds for $(N_5)_6(H_3O)_3(NH_4)_4Cl$.

D-H...A	D-H(Å)	H…A(Å)	D…A(Å)	D-H…A(°)
O(2)-H(2)…N3	0.83(2)	2.26(2)	3.090(4)	180
O(1)-H(1)...N1	0.84(2)	2.17(3)	2.995(3)	168
N(4)-H(4A)...N2	0.82(2)	2.10(2)	2.912(3)	171
N(4)-H(4B)...Cl1	0.83(2)	2.44(2)	3.265(4)	180

Table S5: Torsion angles.

parameter	torsion angle(°)	parameter	torsion angle(°)
N(1)#1-N(1)-N(2)-N(3)	0.000(1)	N(1)-N(2)-N(3)-N(2)#1	0.000(1)

Symmetry code: #1: 1.75-x, 1.75-y, z

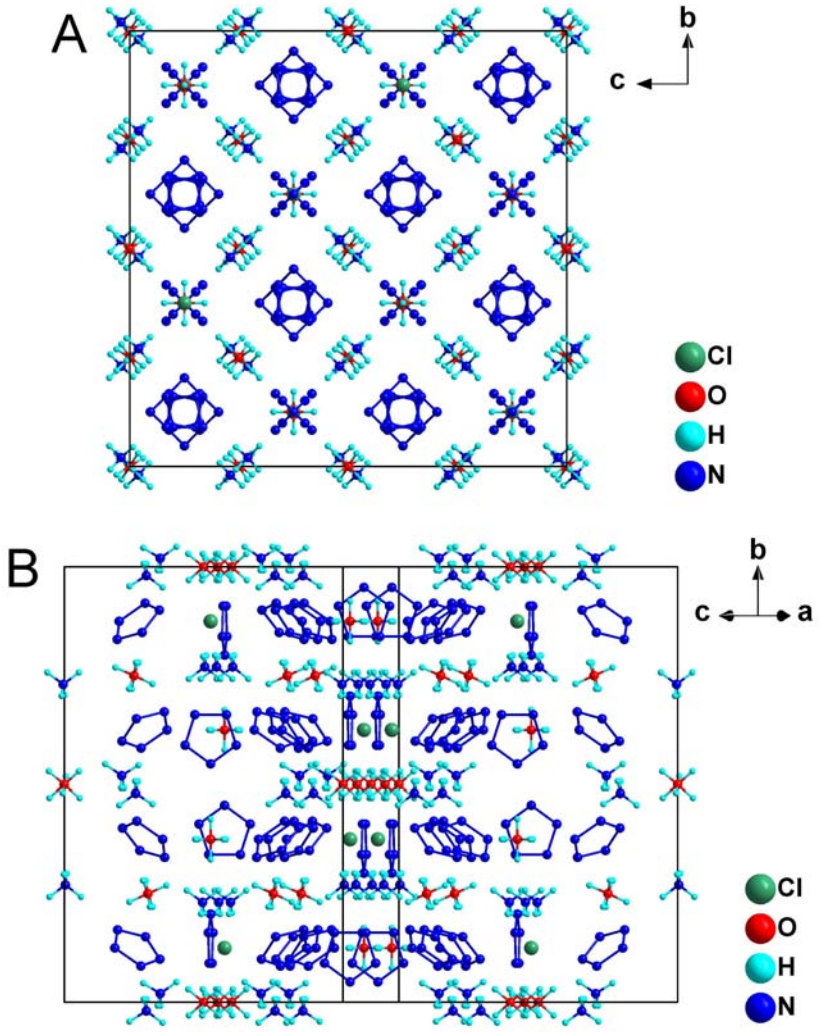

Figure S15: (A) Unit cell view along the *a* axis. (B) Unit cell view along the [605] direction. The unit cell of pentazolate salt contains 192 asymmetric units, each of which consists of 1/24 Cl^-, 1/6 NH_4^+, 1/4 *cyclo*-N_5^-, 1/12 H_3O^+ (O1) and 1/24 H_3O^+ (O2) moieties held together by cation-anion interactions. The Cl^-, NH_4^+, *cyclo*-N_5^-, H_3O^+ (O1) and H_3O^+ (O2) moieties are located on the *b*, *e*, *b*, *d* and *a* Wyckoff positions with multiplicities of 8, 32, 48, 16, 8, respectively. Because of the site symmetry, the O1 position 16*d* and O2 position 8*a* are surrounded by six symmetry-equivalent disordered H1 atoms on position 96*g* and disordered H2 atoms on position 48*f*, respectively, all of which are also assumed to be half-occupied.

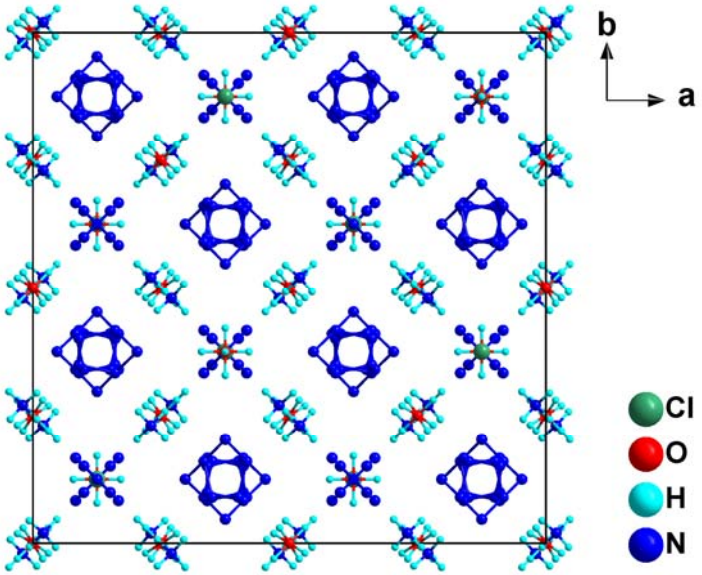

Figure S16: Unit cell view along the *c* axis.

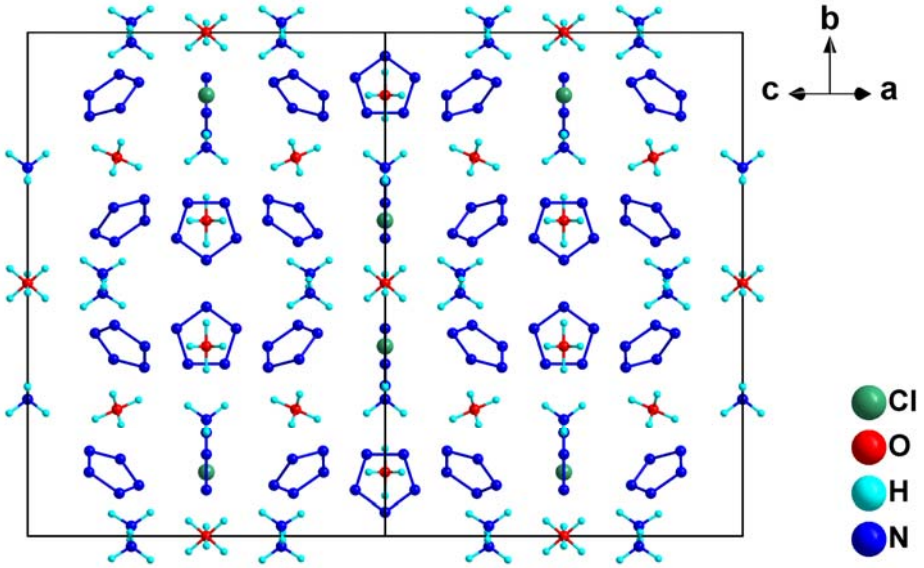

Figure S17: Unit cell view along the [101] direction.

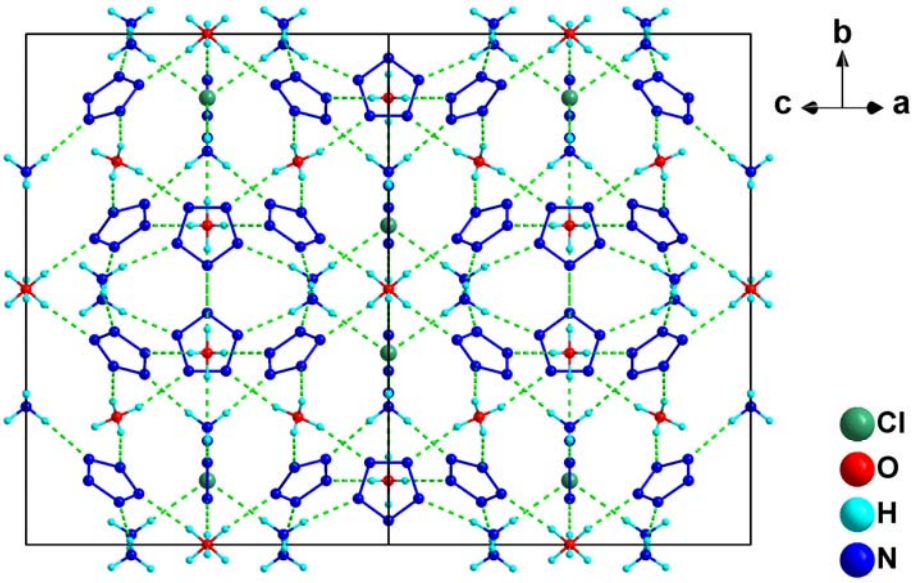

Figure S18: The schematic representation of the hydrogen bonds in the unit cell view along the [101] direction. Ellipsoids are plotted at the 50% probability level. Hydrogen bonds are indicated as green dotted lines.

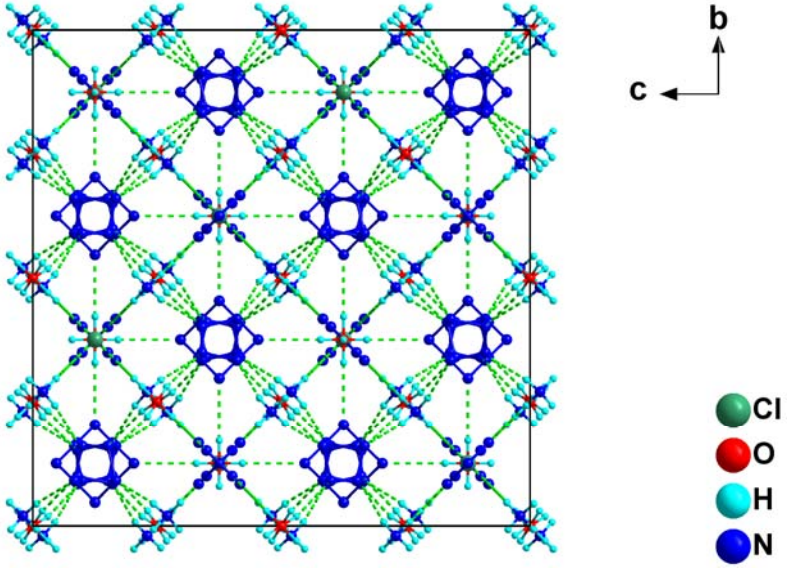

Figure S19: The schematic representation of the hydrogen bonds in the unit cell view along the *a* axis. Ellipsoids are plotted at the 50% probability level. Hydrogen bonds are indicated as green dotted lines.

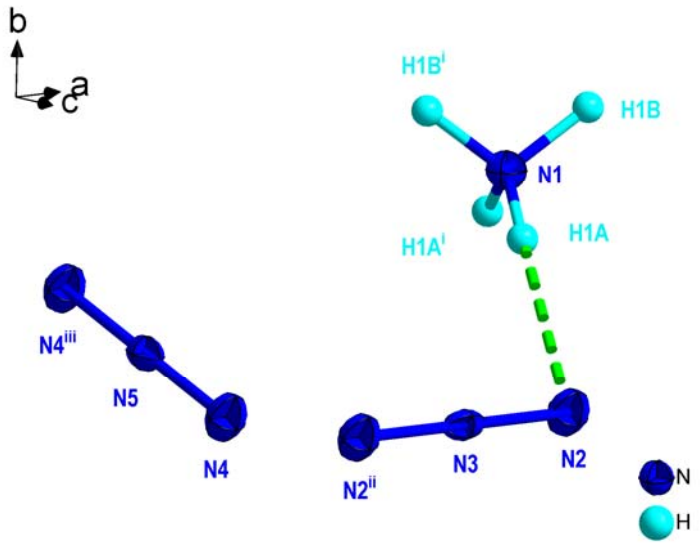

Figure S20: Ellipsoid plot of NH_4N_3 at 50% probability level. The occupancies of NH_4^+, N_3^- are 1/2, 1/4, respectively. Symmetry codes: (i) 1.5-x, y, 0.5-z; (ii) 1-x, 1-y, 1-z; (iii) x, 1-y, z.

References

1. M. Straka, P. Pyykkö, One metal and forty nitrogens. Ab initio predictions for possible new high-energy pentazolides. *Inorg. Chem.* **42**, 8241–8249 (2003). doi:10.1021/ic034702b Medline

2. R. Janoschek, Pentazole and other nitrogen rings. *Angew. Chem. Int. Ed. Engl.* **32**, 230–232 (1993). doi:10.1002/anie.199302301

3. M. T. Nguyen, Polynitrogen compounds. *Coord. Chem. Rev.* **244**, 93–113 (2003). doi:10.1016/S0010-8545(03)00101-2

4. S. Fau, K. J. Wilson, R. J. Bartlett, On the stability of $N_5^+N_5^-$. *J. Phys. Chem. A* **106**, 4639–4644 (2002). doi:10.1021/jp015564j

5. R. N. Butler, A. Fox, S. Collier, L. A. Burke, Pentazole chemistry: The mechanism of the reaction of aryldiazonium chlorides with azide ion at −80°C: Concerted versus stepwise formation of arylpentazoles, detection of a pentazene intermediate, a combined ^{1}H and ^{15}N NMR experimental and ab initio theoretical study. *J. Chem. Soc. Perkin Trans. 2* **10**, 2243–2247 (1998). doi:10.1039/a804040k

6. A. Velian, C. C. Cummins, Synthesis and characterization of $P_2N_3^-$: An aromatic ion composed of phosphorus and nitrogen. *Science* **348**, 1001–1004 (2015). doi:10.1126/science.aab0204 Medline

7. P. Carlqvist, H. Östmark, T. Brinck, The stability of arylpentazoles. *J. Phys. Chem. A* **108**, 7463–7467 (2004). doi:10.1021/jp0484480

8. F. Cacace, G. de Petris, A. Troiani, Experimental detection of tetranitrogen. *Science* **295**, 480–481 (2002). doi:10.1126/science.1067681 Medline

9. A. Vij, J. G. Pavlovich, W. W. Wilson, V. Vij, K. O. Christe, Experimental detection of the pentaazacyclopentadienide (pentazolate) anion, cyclo-N_5^-. *Angew. Chem. Int. Ed.* **41**, 3051–3054 (2002). doi:10.1002/1521-3773(20020816)41:16<3051:AID-ANIE3051>3.0.CO;2-T

10. H. Östmark, S. Wallin, T. Brinck, P. Carlqvist, R. Claridge, E. Hedlund, L. Yudina, Detection of pentazolate anion (cyclo-N_5^-) from laser ionization and decomposition of solid p-dimethylaminophenylpentazole. *Chem. Phys. Lett.* **379**, 539–546 (2003). doi:10.1016/j.cplett.2003.08.081

11. B. Bazanov, U. Geiger, R. Carmieli, D. Grinstein, S. Welner, Y. Haas, Detection of cyclo-N_5^- in THF solution. *Angew. Chem. Int. Ed.* **55**, 13233–13235 (2016). doi:10.1002/anie.201605400 Medline

12. I. Ugi, Pentazole. *Angew. Chem.* **73**, 172 (1961).

13. V. Benin, P. Kaszynski, J. G. Radziszewski, Arylpentazoles revisited: Experimental and theoretical studies of 4-hydroxyphenylpentazole and 4-oxophenylpentazole anion. *J. Org. Chem.* **67**, 1354–1358 (2002). doi:10.1021/jo0110754 Medline

14. R. N. Butler, J. C. Stephens, L. A. Burke, First generation of pentazole (HN_5, pentazolic acid), the final azole, and a zinc pentazolate salt in solution: A new N-dearylation of 1-(p-methoxyphenyl) pyrazoles, a 2-(p-methoxyphenyl) tetrazole and application of the methodology to 1-(p-methoxyphenyl) pentazole. *Chem. Commun.* **8**, 1016–1017 (2003). doi:10.1039/b301491f Medline

15. R. N. Butler, J. M. Hanniffy, J. C. Stephens, L. A. Burke, A ceric ammonium nitrate N-dearylation of *N*-*p*-anisylazoles applied to pyrazole, triazole, tetrazole, and pentazole rings: Release of parent azoles. generation of unstable pentazole, HN_5/N_5^-, in solution. *J. Org. Chem.* **73**, 1354–1364 (2008). doi:10.1021/jo702423z Medline

16. T. Schroer, R. Haiges, S. Schneider, K. O. Christe, The race for the first generation of the pentazolate anion in solution is far from over. *Chem. Commun.* **12**, 1607–1609 (2005). doi:10.1039/b417010e Medline

17. C. Zhang, C. G. Sun, B. C. Hu, M. Lu, Investigation on the stability of multisubstituted arylpentazoles and the influence on the generation of pentazolate anion. *J. Energ. Mater.* **34**, 103–111 (2016). doi:10.1080/07370652.2014.1001918

18. See supplementary materials.

19. H. Shan, Y. Yang, A. J. James, P. R. Sharp, Dinitrogen bridged gold clusters. *Science* **275**, 1460–1462 (1997). doi:10.1126/science.275.5305.1460

20. B. A. Steele, I. I. Oleynik, Sodium pentazolate: A nitrogen rich high energy density material. *Chem. Phys. Lett.* **643**, 21–26 (2016). doi:10.1016/j.cplett.2015.11.008

21. J. D. Wallis, J. D. Dunitz, An all-nitrogen aromatic ring system: Structural study of 4-dimethyl-aminophenylpentazole. *J. Chem. Soc. Chem. Commun.* **16**, 910–911 (1983). doi:10.1039/c39830000910

22. Y. Z. Yang, Y. C. Li, R. B. Zhang, C. H. Sun, S. P. Pang, Thermal stability of p-dimethylaminophenylpentazole. *RSC Advances* **4**, 57629–57634 (2014). doi:10.1039/C4RA08454C

23. S. A. Perera, A. Gregusová, R. J. Bartlett, First calculations of ^{15}N-^{15}N *J* values and new calculations of chemical shifts for high nitrogen systems: A comment on the long search for HN_5 and its pentazole anion. *J. Phys. Chem. A* **113**, 3197–3201 (2009). doi:10.1021/jp809267y Medline

24. C. N. R. Rao, Theory of hydrogen bonding in water. In *Water: A Comprehensive Treatise* (Plenum, 1972), vol. 1, pp. 93–114.

25. G. Marnellos, M. Stoukides, Ammonia synthesis at atmospheric pressure. *Science* **282**, 98–100 (1998). doi:10.1126/science.282.5386.98 Medline

26. S. A. Perera, R. J. Bartlett, Coupled-cluster calculations of Raman intensities and their application to N_4 and N_5^-. *Chem. Phys. Lett.* **314**, 381–387 (1999). doi:10.1016/S0009-2614(99)01186-0

27. A. Nagai, Z. Guo, X. Feng, S. Jin, X. Chen, X. Ding, D. Jiang, Pore surface engineering in covalent organic frameworks. *Nat. Commun.* **2**, 536 (2011). doi:10.1038/ncomms1542 Medline

28. D. A. Dows, G. C. Pimentel, Infrared spectra of gaseous and solid hydrazoic acid and deutero-hydrazoic acid: The thermodynamic properties of HN_3. *J. Chem. Phys.* **23**, 1258–1263 (1955). doi:10.1063/1.1742253

29. D. A. Dows, E. Whittle, G. C. Pimentel, Infrared spectrum of solid ammonium azide: A vibrational assignment. *J. Chem. Phys.* **23**, 1475–1479 (1955). doi:10.1063/1.1742333

30. M. A. Alisi, M. Brufani, N. Cazzolla, F. Ceccacci, P. Dragone, M. Felici, G. Furlotti, B. Garofalo, A. La Bella, O. Lanzalunga, F. Leonelli, R. Marini Bettolo, C. Maugeri, L. M. Migneco, V. Russo, DPPH radical scavenging activity of paracetamol analogues. *Tetrahedron* **68**, 10180–10187 (2012). doi:10.1016/j.tet.2012.09.098

31. P. Müller, R. Herbst-Irmer, A. L. Spek, T. R. Schneider, M. R. Sawaya, *Crystal Structure Refinement: A Crystallographer's Guide to SHELXL* (Oxford Univ. Press, 2006).

32. G. M. Sheldrick, SHELXT—Integrated space-group and crystal-structure determination. *Acta Crystallogr. A* **71**, 3–8 (2015). doi:10.1107/S2053273314026370

33. G. M. Sheldrick, Crystal structure refinement with SHELXL. *Acta Crystallogr. C* **71**, 3–8 (2015). doi:10.1107/S2053229614024218 Medline

34. O. V. Dolomanov, L. J. Bourhis, R. J. Gildea, J. A. K. Howard, H. Puschmann, OLEX2: A complete structure solution, refinement and analysis program. *J. Appl. Crystallogr.* **42**, 339–341 (2009). doi:10.1107/S0021889808042726